

Quantum version of the Euler's problem: a geometric perspective

Karol Życzkowski^{1,2}

¹*Institute of Theoretical Physics, Jagiellonian University,
ul. Łojasiewicza 11, 30-348 Kraków, Poland and*

²*Center for Theoretical Physics, Polish Academy of Sciences, Aleja Lotników 32/46, 02-668 Warsaw, Poland
(Dated: December 23, 2022)*

The classical combinatorial problem of 36 officers has no solution, as there are no Graeco-Latin squares of order six. The situation changes if one works in a quantum setup and allows for superpositions of classical objects and admits entangled states. We analyze the recently found solution to the quantum version of the Euler's problem from a geometric point of view. The notion of a *non-displaceable manifold* embedded in a larger space is recalled. This property implies that any two copies of such a manifold, like two great circles on a sphere, do intersect. Existence of a quantum Graeco-Latin square of size six, equivalent to a maximally entangled state of four subsystems with $d = 6$ levels each, implies that *three* copies of the manifold $U(36)/U(1)$ of maximally entangled states of the 36×36 system, embedded in the complex projective space $\mathbb{C}P^{36 \times 36 - 1}$, do intersect simultaneously at a certain point.

Dedicated to the memory of Bogdan Mielnik

I. INTRODUCTION

Quantum information processing takes place in laboratory [1]. To describe such a process from a theoretical point of view it is convenient to use the notion of a density matrix ρ and the set Ω_d of all quantum states of size d . As emphasized in pioneering papers by Mielnik [2, 3], the most important feature of this set is its convexity.

Extremal points of the convex set Ω_d are formed by projectors on the pure quantum states, $P_\psi = |\psi\rangle\langle\psi|$. Any pure state corresponds to a vector in a complex Hilbert space, $|\psi\rangle \in \mathcal{H}_d$, normalized as $\langle\psi|\psi\rangle = 1$. As the global phase α is not measurable it is sufficient to analyze equivalence classes, $|\psi\rangle \sim e^{i\alpha}|\psi\rangle$, which form a complex projective space $\mathbb{C}P^{d-1}$ of $2(d-1)$ real dimension.

In the simplest case of a single-qubit system, $d = 2$, the space of pure states forms the Bloch sphere, $S^2 = \mathbb{C}P^1$. Although for higher d the complex projective space $\mathbb{C}P^{d-1}$ is not equivalent to a hypersphere, it enjoys the same homogeneity property: There are no privileged points as all its points are alike.

The situation changes if a certain structure is imposed to the system. Consider, for instance, a nine dimensional system described by a state $|\psi\rangle \in \mathcal{H}_9$. Assume that it is physically justified to distinguish two subsystems of size three, and identify a two-qutrit system $\mathcal{H}_9 = \mathcal{H}_3 \otimes \mathcal{H}_3 = \mathcal{H}_A \otimes \mathcal{H}_B$, where integers in indices denote the dimensionality of subsystems, which are labeled by capital letters. With respect to a given splitting of the composed Hilbert space, $\mathcal{H}_{AB} = \mathcal{H}_A \otimes \mathcal{H}_B$, one defines *separable* states, which have the tensor product structure, $|\psi_{\text{sep}}\rangle = |\phi_A\rangle \otimes |\phi_B\rangle$. Note that a partial trace of the projector $|\psi_{\text{sep}}\rangle\langle\psi_{\text{sep}}|$ is pure, so its rank $r = 1$.

All other states, with reduced state $\sigma_A = \text{Tr}_B |\psi_{AB}\rangle\langle\psi_{AB}|$ of rank $r \geq 2$ are called *entangled*. If the partial trace σ_A is proportional to identity, the state $|\psi_{AB}\rangle$ is called *maximally entangled*. These states, for a

two-qubit system called *Bell states*, play a crucial role in the theory of quantum information processing [4]. The structure of the manifolds of separable and maximally entangled states pure for a bi-partite $d \times d$ systems is well understood [5].

On the other hand, for multipartite systems, described in the Hilbert space with several factors, $\mathcal{H}_A \otimes \mathcal{H}_B \otimes \dots \otimes \mathcal{H}_N$, the notion of extremal entanglement is not unique [6, 7], as it depends on the measure selected [8, 9].

If the number N of subsystems is even, one defines *absolutely maximally entangled* (AME) states, as these which are maximally entangled for all symmetric partitions [10]. In the case of $N = 4$ subsystems $ABCD$ one needs to verify that three bipartite reduced states, σ_{AB} , σ_{AC} and σ_{AD} are maximally mixed. In a seminal paper of Higuchi and Sudbery it was proved that in the case of a four-qubit system, $N = 4$ and $d = 2$, there are no AME states [11]. However, for some other values of the parameters N and d , such pure quantum states with extremal properties are known [8, 9] and they find applications in certain quantum protocols [10].

There are useful relations between classical combinatorial designs [12] and strongly entangled multipartite quantum states [13, 14]. The existence of two mutually orthogonal Latin squares (MOLS) [15] of order d , also called *Graeco-Latin squares*, implies existence of AME states of $N = 4$ subsystems with d levels each, written $\text{AME}(4, d)$. As these designs exist for $d = 3, 4, 5$ and any $d \geq 7$ – see [15, 16], it is possible to construct states $\text{AME}(4, d)$ for these dimensions.

In dimension $d = 6$, the smallest number which is neither a prime nor a power of prime, there are no Graeco-Latin squares (another name of MOLS), as conjectured by Euler and proved by Tarry [17, 18]. Hence the problem, whether there exist $\text{AME}(4, 6)$ state was open until very recently [19–21].

The goal of the present contribution is to analyze the recent solution of the quantum analogue of the Euler problem of 36 officers [22, 23] from a geometric perspective. In the next section the structure of the manifolds of

separable and maximally entangled states of a bipartite system is reviewed. The notion of non-displaceable manifolds is recalled in Sec. III and a conjecture concerning mutually maximally entangled states for a $d \times d$ system is presented. Absolutely maximally entangled states for multipartite systems are discussed in Sec. IV, their link to orthogonal Latin squares is analyzed in Sec. V, while quantum orthogonal Latin squares are recalled in Sec. VI.

In Sec. VII we show some consequences of the fact that a solution of the quantum version of the problem of 36 officers of Euler does exist. It implies existence of an AME state of a four-partite system $ABCD$ with $d = 6$ levels each, which in turn implies that the intersection of three copies of manifolds $PU(36) = U(36)/U(1)$ of maximally entangled bi-partite states, corresponding to partitions $AB|CD$ and $AC|BD$ and $AD|BC$, embedded in the complex projective space $\mathbb{C}P^{36 \times 36 - 1}$, is not empty. As such four-qubit AME states do not exist, for $d = 2$ analogous three manifolds $U(4)/U(1)$ embedded in $\mathbb{C}P^{4 \times 4 - 1}$ do not intersect in a single point. Key mathematical notions used in this work are listed in Appendix A.

II. SEPARABLE AND MAXIMALLY ENTANGLED STATES OF A BIPARTITE $d \times d$ QUANTUM SYSTEM

Consider a pure quantum state of a $d \times d$ bipartite system, $|\psi\rangle \in \mathcal{H}_A \otimes \mathcal{H}_B$. Let $\mathcal{P}_{d^2} = \mathbb{C}P^{d^2 - 1}$ denote the space of pure quantum states of this system. It has $2(d^2 - 1)$ real dimensions. Introducing a product basis $|i, j\rangle = |i\rangle \otimes |j\rangle$ with $i, j = 1, \dots, d$, one can write any state as a double sum, arranging the coefficients into a complex matrix C ,

$$|\psi\rangle = \sum_{i,j=1}^d C_{ij} |i\rangle \otimes |j\rangle = \sum_{i=1}^r \sqrt{\lambda_i} |i'\rangle \otimes |i''\rangle, \quad (1)$$

where $r \leq d$ denotes the rank of C . The second form with a single sum, known as the *Schmidt decomposition* of $|\psi\rangle$, involves singular values $\sqrt{\lambda_i}$ of the matrix C . Thus $\lambda_i \geq 0$ represent eigenvalues of a positive semidefinite matrix CC^\dagger , while the rotated basis $|i', i''\rangle$, is determined by the eigenvectors of CC^\dagger and $C^\dagger C$. The standard normalization condition, $\|\psi\|^2 = 1$, implies $\|C\|^2 = \text{Tr}CC^\dagger = 1$, so that the Schmidt coefficients form a probability vector Λ , with $\sum_{i=1}^d \lambda_i = 1$.

A separable state $|\psi_{\text{sep}}\rangle$, is by definition represented by the ordered vector $\Lambda = (\lambda_1 \geq \lambda_2 \geq \dots \geq \lambda_d) = (1, 0, \dots, 0)$. Any state with $r \geq 2$ positive Schmidt coefficients is called *entangled*, so the scaled rank of a matrix, $(r(C) - 1)/(d - 1)$, can serve as a rough measure of entanglement. To get a better characterization one often uses the *entanglement entropy*, $S(|\psi\rangle) = S(\Lambda) = -\sum_{i=1}^d \lambda_i \ln \lambda_i$, that vanishes for separable states, $S(|\psi_{\text{sep}}\rangle) = 0$. Any bipartite state with

$\Lambda = (1, 1, \dots, 1)/d$ is called *maximally entangled*, as it corresponds to the maximal entanglement entropy, $S(|\psi_{\text{max}}\rangle) = \ln d$. In this case the partial trace of the projector, $\rho_\psi = |\psi\rangle\langle\psi|$, is maximally mixed, $\text{Tr}_B \rho_\psi = CC^\dagger = \mathbb{I}/d$, and the same is true for the dual reduction, $\text{Tr}_A \rho_\psi = C^\dagger C = \mathbb{I}/d$. Hence an equivalent condition for maximal degree of mixing is that the matrix of coefficients is proportional to a unitary, $C = V/\sqrt{d}$ such that $VV^\dagger = \mathbb{I}_d$.

Let $U_{\text{loc}} = U_A \otimes U_B$ denote a *local unitary* (LU), as $U_A, U_B \in U(d)$ and $U_{\text{loc}} \in U(d^2)$. The Schmidt decomposition (1) implies that the Schmidt vector Λ and the entropy function $S(\Lambda)$ are invariant with respect to local unitaries: two locally equivalent bi-partite states, $|\psi_{AB}\rangle \sim_{LU} |\psi'_{AB}\rangle = U_A \otimes U_B |\psi_{AB}\rangle$, share the same amount of entanglement.

In the simplest case of a two-qubit system, $d = N = 2$, the maximal entanglement is characteristic to the Bell state,

$$|\psi_{\text{Bell}}\rangle = \frac{1}{\sqrt{2}} (|1, 1\rangle + |2, 2\rangle), \quad (2)$$

which exhibits perfect correlations between results of measurement in subsystems A and B . It is easy to check that both partial traces are maximally mixed, so having perfect knowledge about the state of a composed system one has no information about its parts. Observe that the state $|\psi_{\text{H}}\rangle = (|1, 1\rangle + |1, 2\rangle + |2, 1\rangle - |2, 2\rangle)/2$ is maximally entangled, as the matrix C is proportional to the unitary Hadamard matrix H_2 , so it is locally equivalent to the Bell state.

The set of separable states, written \mathcal{P}_{sep} , contains states of the form, $(U_A \otimes U_B)(|\phi_A\rangle \otimes |\phi_B\rangle)$, which correspond to independent events in the classical theory of probability. The set of separable states of real dimension $4(d - 1)$ is thus given by the Cartesian product, which forms the Segre embedding,

$$\mathcal{P}_{\text{sep}} = \mathbb{C}P^{d-1} \times \mathbb{C}P^{d-1} \subset \mathbb{C}P^{d^2-1}. \quad (3)$$

In the case of a two-qubit system, $d = 2$, one has $\mathbb{C}P^1 = S^2$, so it is just an embedding of the product of two spheres, $S^2 \times S^2 \subset \mathbb{C}P^3$.

Any maximally entangled state can be obtained from the generalized Bell state by a local rotation, $|\psi_{\text{max}}\rangle = (U_A \otimes \mathbb{I}) \frac{1}{\sqrt{d}} \sum_{i=1}^d |i, i\rangle$. An equivalent expression is obtained by applying the local transformation $(\mathbb{I} \otimes U_B)$. As any global phase, $e^{i\alpha} \in U(1)$, does not influence the state, the set of maximally entangled states, of real dimension $d^2 - 1$, has the structure of the manifold corresponding to the projective unitary group [5],

$$\mathcal{P}_{\text{max}} \cong PU(d) = U(d)/U(1) \subset \mathbb{C}P^{d^2-1}. \quad (4)$$

Figure 1 shows a scheme of the 6-dimensional space \mathcal{P}_4 of pure states for a two-qubit system. A simple two dimensional sketch shown in Fig. 1a cannot be precise: on one hand the set \mathcal{P}_{max} of maximally entangled states

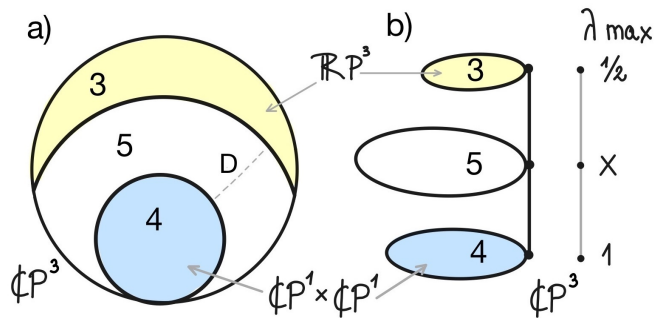


FIG. 1: Set of pure states for two-qubit system, $\mathcal{P}_4 = \mathbb{C}P^3$. a) Sketch shows the subset of maximally entangled states, $\mathcal{P}_{\max} = PU(2) = U(2)/U(1) = \mathbb{R}P^3$, located at the maximal Fubini-Study distance $D = \arccos(1/\sqrt{2}) = \pi/4$ from the product of two spheres, forming the set of separable states, $\mathcal{P}_{\text{sep}} = S^2 \times S^2 \subset \mathbb{C}P^3$. Panel b) shows its foliation into local orbits labeled by the Schmidt vector $\Lambda = (x, 1-x)$. For a generic value of x the local orbit has 5 real dimensions.

is located ‘as far’ as possible from the Cartesian product of two Bloch spheres, forming the set \mathcal{P}_{sep} of separable states. On the other hand, for any dimension d , the set \mathcal{P}_{\max} should not be situated ‘at the boundary’ of the set \mathcal{P}_{d^2} , as it corresponds to the center $\Lambda_* = (1, 1, \dots, 1)/d$ of the simplex of the Schmidt vectors, while separable states form an orbit which connects its all corners, $\Lambda = (1, 0, \dots, 0)$.

Fig. 1b shows a foliation of $\mathbb{C}P^3$ generated by the Schmidt coefficients: any point x from $[1/2, 1]$ generates an orbit of locally equivalent states,

$$|\psi_x\rangle = (U_A \otimes U_B)[\sqrt{x}|11\rangle + \sqrt{1-x}|22\rangle]. \quad (5)$$

A generic orbit corresponding to $x \in (1/2, 1)$ has 5 dimensions and the structure $\frac{U(2)}{[U(1)]^2} \times \mathbb{R}P^3$. For $x = 1/2$ the manifold of maximally entangled states, $\mathcal{P}_{\max} = U(2)/U(1)$, has 3 dimensions, while the stratum of separable states $\mathcal{P}_{\text{sep}} = \mathbb{C}P^1 \times \mathbb{C}P^1$ at $x = 1$ has 4 dimensions.

For any higher dimension d it is not simple to understand the geometry of the space $\mathcal{P}_{d^2} = \mathbb{C}P^{d^2-1}$ of pure states of a two-qudit system, with embedded subspaces $\mathcal{P}_{\text{sep}} = \mathbb{C}P^{d-1} \times \mathbb{C}P^{d-1}$ of separable states and $\mathcal{P}_{\max} = PU(d) = U(d)/U(1)$ of maximally entangled states. One can apply the notion of the numerical range of an operator of order d^2 , which gives a projection of the entire projective space $\mathbb{C}P^{d^2-1}$ onto a plane [24] and their variants including entangled and separable numerical ranges [25], but these projections do depend on the operator selected and do not always lead to a clear visualization of the manifold projected.

Therefore, inspired by the recent work [26], which presents a nice way to elucidate the structure of the eight dimensional set Ω_3 of mixed states of a qutrit, in Fig. 2 we set $d = 3$ and show a sketch of the foliation of the

space $\mathcal{P}_9 = \mathbb{C}P^8$ of pure states for two qutrits into local orbits. Consider the simplex of Schmidt coefficients of a bipartite state $|\psi_{AB}\rangle \in \mathcal{H}_9$, which describes also the spectrum of both partial traces. The orbit of separable states, $\mathcal{P}_{\text{sep}} = \mathbb{C}P^2 \times \mathbb{C}P^2$, connecting all three corners of the simplex, has $4 + 4 = 8$ real dimensions. In this case also the manifold $\mathcal{P}_{\max} = PU(3)$ of maximally entangled states, originating from the center of the simplex $\Lambda_* = \frac{1}{3}(1, 1, 1)$, has $9 - 1 = 8$ real dimensions. Analyzing foliation of the projective space \mathcal{P}_9 with respect to the base formed by the simplex Δ_3 of the Schmidt coefficients the manifold \mathcal{P}_{\max} sits ‘just its the center’ and its distance to \mathcal{P}_{sep} reads $D = \arccos(1/\sqrt{3})$ – see Fig. 2. A generic orbit, stemming from a typical point of the simplex with rank two, $(x, y, 1-x-y)$, contains states

$$|\psi_{x,y}\rangle = (U_A \otimes U_B)[\sqrt{x}|11\rangle + \sqrt{y}|22\rangle + \sqrt{1-x-y}|33\rangle]. \quad (6)$$

Such an orbit of locally equivalent states has the structure $[U(3)/U(1)] \times [U(3)/U(1)]^{\times 3}$ and $8 + 6 = 14$ dimensions [5].

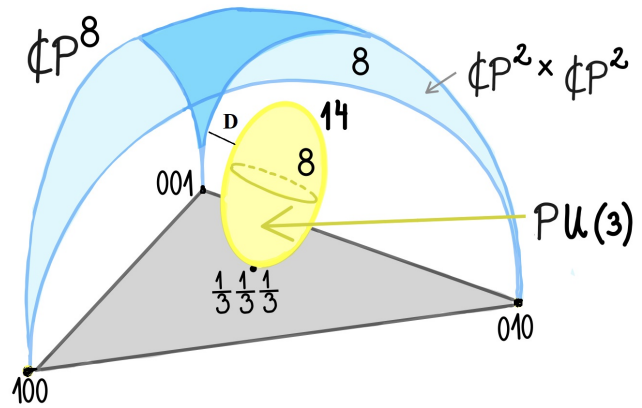


FIG. 2: Foliation of 16 dimensional set $\mathcal{P}_9 = \mathbb{C}P^8$ of pure states for a 3×3 system induced by the simplex Δ of Schmidt vectors: the set of product states, $\mathbb{C}P^2 \times \mathbb{C}P^2$, connecting three corners of the simplex, has 8 dimensions. The antipodal subset, $\mathcal{P}_{\max} = PU(3) = U(3)/U(1)$, of maximally entangled states, which emerges from the center of the simplex is of the same dimensionality. Any generic orbit is 14 dimensional.

III. NON-DISPLACEABLE MANIFOLDS AND MUTUALLY ENTANGLED STATES

A pure state of a system described in a Hilbert space of dimension d^2 is called separable with respect to a particular splitting of the Hilbert space, $\mathcal{H}_{d^2} = \mathcal{H}_d \otimes \mathcal{H}_d = \mathcal{H}_A \otimes \mathcal{H}_B$, if it has a product form, $|\phi_A\rangle \otimes |\phi_B\rangle$. A state $|\psi_{\text{sep}}\rangle$, separable with respect to the partition $\mathcal{H}_A \otimes \mathcal{H}_B$, needs not to be separable with respect to any other partition, $\mathcal{H}_{d^2} = \mathcal{H}_{A'} \otimes \mathcal{H}_{B'}$, obtained from the initial one by a global unitary transformation $U \in U(d^2)$. The same property concerns maximal entanglement: a state $|\psi_{\max}\rangle$,

maximally entangled with respect to the partition $A|B$ is not necessarily maximally entangled with respect to another partition $A'|B'$.

We are going to analyze *mutually entangled* states [27], which are maximally entangled with respect to two given partitions $A|B$ and $A'|B'$. For this purpose, it is convenient to use the notion of *non-displaceable manifolds*. Such a manifold embedded in a larger space has a particular feature that it cannot be displaced into any other position, in a way, that the original manifold and the displaced one do not intersect [28, 29].

Consider an equator S^1 of a standard two-sphere which contains points equally distant from both poles N and S . It is easy to see that this manifold is non-displaceable in S^2 , as any two great circles of a sphere do intersect. These two mutually antipodal intersection points belong simultaneously to both great circles, and their geodesic distances to the original poles N, S of the sphere and to the rotated poles, N' and S' , are equal – see Fig. 3.

The above statement can be formulated more precisely as

a) a great circle S^1 embedded in S^2 is not displaceable with respect to $O(3)$ transformations.

This simple fact can be generalized for higher dimensions in various ways and concerns Lagrangian submanifolds of a space with a symplectic structure.

b) a Clifford torus T^M (flat embedding of the Cartesian product of M great circles) embedded in a complex projective space $\mathbb{C}P^M$ is non-displaceable with respect to transformations by a unitary $U \in U(M+1)$ – see [28, 29];

c) the real projective space $\mathbb{R}P^M$ is non-displaceable in $\mathbb{C}P^M$ with respect to transformations by $U(M+1)$ [29, 30].

Observe that in analogy to case a) also in cases b)–c) the dimension M of the non-displaceable manifold is equal to half of the real dimension $2M$ of the embedding space. These mathematical results find their direct applications in quantum physics. Since a great torus T^M is non-displaceable in a complex projective space $\mathbb{C}P^M$, for any choice of two fixed bases in \mathcal{H}_{M+1} there exist quantum states *mutually coherent*, as their coherences with respect to both bases are maximal [31]. Analyzing the intersection points of any two Clifford tori T^M is interesting from the point of view of mutually unbiased bases and characterization of the set of unistochastic matrices [32].

As discussed in the previous section, for a two-qubit system, the set of maximally entangled states reads, $\mathcal{P}_{\max} = U(2)/U(1) = SU(2)/Z_2$, where Z_2 denotes the finite group of order two. Making use of a homomorphism between classical groups, $SU(2) \sim SO(3)$, one has $\mathcal{P}_{\max} = O(3)/O(2) = \mathbb{R}P^3$. As a real projective space embedded in the complex projective space is not displaceable – see item c) above, for any global unitary matrix $U \in U(4)$, which determines the transformed partition

$A'|B'$, there exists a mutually entangled state, maximally entangled with respect to both partitions [27].

The following generalization, based on numerical results, was conjectured in [27]: for any two splittings $A|B$ and $A'|B'$ of the $d \times d$ quantum system, related by an arbitrary $U \in U(d^2)$, there exist a *mutually entangled* state, maximally entangled with respect to both partitions. From a geometric perspective this statement is equivalent to

d) manifold corresponding to projective unitary space, $PU(d) = U(d)/U(1)$, is *conjectured to be* non-displaceable in $\mathbb{C}P^{d^2-1}$ with respect to transformations by $U(d^2)$,

which has not been proven, so far.

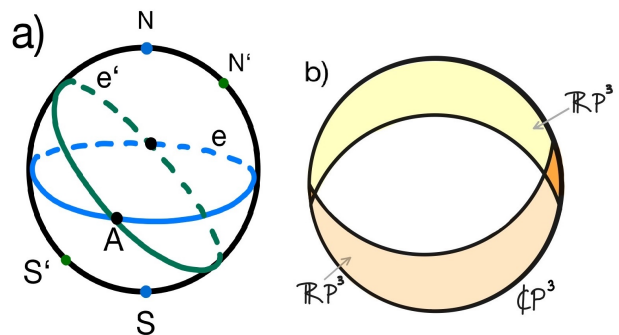


FIG. 3: a) Equator S^1 is non-displaceable in S^2 as two great circles on a sphere e and e' do intersect; b) the set of maximally entangled two-qubit states, $\mathcal{P}_{\max} = PU(2) = \mathbb{R}P^3$, is non-displaceable in the set of all pure states, $\mathcal{P}_4 = \mathbb{C}P^3$, so mutually entangled states do exist in this case.

IV. MULTIPARTITE SYSTEMS AND ABSOLUTELY MAXIMALLY ENTANGLED STATES

Any quantum system consisting of N subsystems can be described in a Hilbert space composed of N factors, $\mathcal{H} = \mathcal{H}_A \otimes \mathcal{H}_B \otimes \cdots \otimes \mathcal{H}_N$. Assuming, for simplicity, that all local dimensions are equal to d , the entire space has d^N complex dimensions. Any pure state $|\psi\rangle \in \mathcal{H}$ can be represented in a product basis by a tensor T with N indices, each running from 1 to d ,

$$|\psi\rangle = \sum_{i_1, \dots, i_N=1}^d T_{i_1, i_2, \dots, i_N} |i_1\rangle \otimes |i_2\rangle \otimes \cdots \otimes |i_N\rangle. \quad (7)$$

In analogy to the bi-partite case, such a state is separable if the tensor T is of rank one, so there exists a product basis in which the above sum reduces to a single term only. In the bi-partite case, $N = 2$ the tensor T reduces to a matrix, denoted in Eq. (1) by C , for which it is simple to find its rank r , its norm and to perform

its singular value decomposition. In general, for a tensor with $N \geq 3$ indices, there is no direct analogue of singular value decomposition [33–35], and even evaluation of a rank of a tensor (there are various variants of this notion!) becomes difficult [36–38].

To characterize the degree of entanglement quantitatively one can apply geometric measures of entanglement, initially developed for bipartite systems [39–41], and generalize them for a multipartite scenario [42]. In short, entanglement of a given state $|\psi\rangle$ can be defined by its distance D_{\min} to the closest separable state $|\phi_{\text{sep}}\rangle \in [\mathbb{C}P^{d-1}]^{\times N}$. Using the natural geodesic distance on the complex projective space, equivalent to the Fubini-Study distance, one gets a simple expression, $D_{\min}(\psi) = \arccos(|\langle\psi|\phi_{\text{sep}}\rangle|)$, but the problem consists in identification of the closest separable state, which is often difficult.

In the bipartite case (1), the overlap is determined by the largest singular value of the matrix C of coefficients, $|\langle\psi|\phi_{\text{sep}}\rangle| = \sqrt{\lambda_{\max}}$, equal to the spectral norm $\|C\|_{\infty}$. For a multipartite system, this generalizes directly [43] to the spectral norm $\|T\|_{\infty}$ of a tensor [44]. Alternatively, the degree of entanglement can be also characterized by the nuclear norm $\|T\|_1$ of a tensor, dual to the spectral norm, but evaluation of both quantities is hard [45]. To overcome cumbersome problems with tensor algebra one can investigate multipartite entanglement by studying bipartite entanglement for various splittings [8, 9, 46].

An interesting class of highly entangled N -partite states is called k -uniform [8, 47]. Such a state $|\psi_N\rangle \in \mathcal{H}_d^{\otimes N}$ is distinguished by the following condition: for any choice of k out of N subsystems, the reduced density matrix, obtained by partial trace over the remaining $N - k$ subsystems, is maximally mixed,

$$\rho_k = \text{Tr}_{N-k} |\psi_N\rangle\langle\psi_N| \propto \mathbb{I}_{d^k}. \quad (8)$$

This implies that for any choice of k subsystems quantum correlations between them and the remaining $N - k$ subsystems are maximal. As the rank of a partial trace of an $d_1 \times d_2$ bipartite system is not larger than $\min(d_1, d_2)$, property (8) can hold if the number k of remaining subsystems is not larger than $N - k$. Hence the maximal degree of uniformity of an N -party pure state is $k_{\max} = \lfloor N/2 \rfloor$. Therefore such multipartite states are called *absolutely maximally entangled* (AME) [10], as they display extremal bi-partite correlations among all possible splittings.

It is known that there are no such states for $N = 4$ qubits [11, 48], but such states exist for five and six qubits. Furthermore, by increasing the local dimension one can find AME states of four qutrits – subsystems with local dimension $d = 3$, first analyzed by Popescu,

$$\begin{aligned} |\text{AME}(4, 3)\rangle = & |1111\rangle + |1223\rangle + |1332\rangle + \\ & |2122\rangle + |2231\rangle + |2313\rangle + \\ & |3133\rangle + |3212\rangle + |3321\rangle, \end{aligned} \quad (9)$$

where the normalization constant is omitted for brevity. Allowing the indices to run from 0 to $d - 1$ the same state

can be written in a more compact form,

$$|\text{AME}(4, 3)\rangle = \sum_{i,j=0}^2 |i\rangle|j\rangle|i \oplus j\rangle|i \oplus 2j\rangle, \quad (10)$$

where addition \oplus inside the kets is understood modulo $d = 3$. It is easy to check that this state possesses the required properties as it is $k = 2 = N/2$ uniform – all partial traces of the projector over any two subsystems are maximally mixed, so the quantum correlations between all four subsystems are maximal.

Further examples for $d = 4, 5$ and $d \geq 7$ can be generated from classical combinatorial designs called mutually orthogonal Latin squares as described in Section V. A list of dimensions d and numbers of subsystems N , for which states $\text{AME}(N, d)$ exist [49] is also available online [20].

Let us concentrate here on the case $N = 4$, such that any pure state $|\psi\rangle$ is represented in (7) by a tensor T_{ijkl} with four indices, each running from 1 to d , which are related to four subsystems, $ABCD$. Three possible symmetric splittings of the system, $AB|CD$, $AC|BD$ and $AD|BC$, correspond to three different flattenings of the tensor T_{ijkl} into matrices $T_{\mu\nu}$ of order d^2 , where both composed indices, $\mu, \nu = 1, \dots, d^2$, are obtained by grouping together two out of four initial indices i, j, k, ℓ .

As discussed in Section II maximal entanglement of any bi-partite, $d \times d$ state requires that the matrix of coefficients is unitary, up to rescaling $CC^\dagger = \mathbb{I}/d$. Thus a 4-party AME state, satisfies simultaneously unitarity conditions for three different splittings: the matrices $X_{\mu\nu} = T_{ij,k\ell}$, $Y_{\mu\nu} = T_{ik,j\ell}$, $Z_{\mu\nu} = T_{i\ell,kj}$, with index μ determined by a) pair (i, j) ; b) pair (i, k) , and c) pair (i, ℓ) , are unitary up to a constant. A four-index tensor T_{ijkl} with the property that its three flattenings are proportional to a unitary is called *perfect* [50]. The resulting unitary matrix $U = Xd$ of size d^2 with the property that its both reorderings Yd and Zd are also unitary, is called *two-unitary* [14]. These reorderings of entries of the matrix, induced by permutations of indices of dT_{ijkl} , are often called reshuffling and partial transpose, written as $U^R = Yd$ and $U^\Gamma = Zd$ respectively, see [22, 51].

Observe that a change of the partition $AB|CD$ into $AC|BD$, corresponds to a different choice of a pair of indices of the tensor T_{ijkl} , and also to a unitary permutation of order d^4 , which induces a transformation of the subspace \mathcal{P}_{\max} of maximally entangled states of the bipartite, $d^2 \times d^2$ system. It is thus natural to refer to the theory of non-displaceable manifolds, discussed in Sec. III. The conjectured property d) implies that arbitrary ‘two copies’ of the manifold $\mathcal{P}_{\max} = PU(d^2)$ do intersect in the embedding space \mathcal{P}_{d^4} . However, this fact does not imply the AME property, which requires *three* concrete ‘copies’ of this manifold, corresponding to three different splittings of the system, do intersect in a single point.

The work by Higuchi and Sudbery [11] implies that the dimension $d = 2$ is ‘not big enough’ to allow for the existence of AME states of four qubits. Let us illustrate this

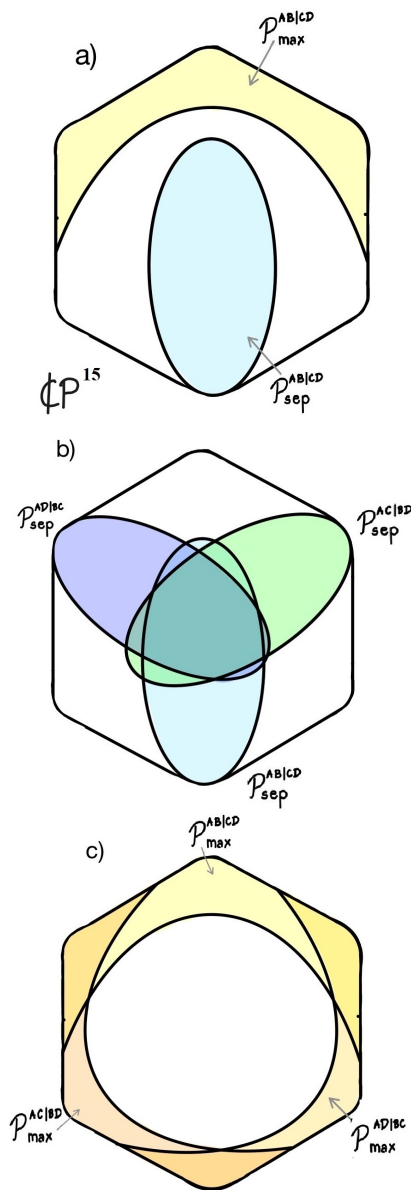


FIG. 4: Four-qubit system $ABCD$ can be treated as a bipartite, two-ququart systems in three different ways: a) shows the sets of separable $\mathcal{P}_{\text{sep}}^{AB|CD} \subset \mathcal{P}_{16}$ and maximally entangled states, $\mathcal{P}_{\text{max}}^{AB|CD}$, for a selected splitting; states separable with respect to three different splittings are shown in panel b), while panel c) presents analogous sketch for maximally entangled states $\mathcal{P}_{\text{max}} = PU(4) = U(4)/U(1)$. Note that any two sets \mathcal{P}_{max} do intersect, but the intersection of all three of them is empty.

fact in terms of intersections of manifolds of maximally entangled states for this 4-party system, treated here as a bi-partite, $d^2 \times d^2$ system.

In principle, one could follow the scheme of [26], and in analogy to Fig. 2, consider a tetrahedron of Schmidt coefficients of a 4×4 pure states, plot the orbit of separable states, $\mathcal{P}_{\text{sep}} = \mathbb{C}P^3 \times \mathbb{C}P^3$, which connects four corners

of the simplex, and place the manifold $\mathcal{P}_{\text{max}} = PU(4)$ of maximally entangled states, at the center of the tetrahedron, $\Lambda_* = \frac{1}{4}(1, 1, 1, 1)$. However, as we need to consider three different splittings of a four-party system $ABCD$, Fig. 4 is constructed in analogy to Fig. 1 representing pure states for a two-qubit system.

In Fig. 4a) we show the set of states which are separable, $\mathcal{P}_{\text{sep}}^{AB|CD}$, and maximally entangled, $\mathcal{P}_{\text{max}}^{AB|CD}$, with respect to this splitting $AB|CD$ of the system. Both sets are located at the distance $D = \arccos(1/2) = \pi/3$ apart. Further panels show analogous sets for other splittings. Three copies of the set \mathcal{P}_{sep} do intersect in the center of Fig. 4b), as any fully separable state, $|\phi_A\rangle \otimes |\phi_B\rangle \otimes |\phi_C\rangle \otimes |\phi_D\rangle$, is manifestly separable with respect to all three splittings. As the set $\mathcal{P}_{\text{max}} = PU(4)$ is conjectured to be non-displaceable in \mathcal{P}_{16} two copies of this set do intersect. However, the joint intersection of three such copies is empty as sketched in Fig. 4c), since there are no AME(4, 2) states.

V. CLASSICAL ORTHOGONAL LATIN SQUARES

A classical combinatorial design consists of discrete symbols arranged with a particular ‘symmetry and balance’ [12]. A simple example is provided by a *Latin square* of order d , which consists d copies of d symbols, arranged into a square of size d in such a way, that each row and each column contains different symbols. It is easy to see that such configurations exist for any dimension d .

Leonhard Euler analyzed such designs and became interested in constructing pairs of Latin squares that satisfy an additional condition of *orthogonality*: all possible pairs of d^2 symbols are present in the square. A pair of orthogonal Latin squares is also called a *Graeco-Latin square*, since Euler represented one square with Greek letters and the other one with Latin. A simple example of such a pattern, written OLS(3), i.e. orthogonal Latin squares of order three, is shown in Fig.5.

αA	βC	γB	$A\spadesuit_1$	$K\clubsuit_2$	$Q\diamond_3$
βB	γA	αC	$K\diamond_4$	$Q\spadesuit_5$	$A\clubsuit_6$
γC	αB	βA	$Q\clubsuit_7$	$A\diamond_8$	$K\spadesuit_9$

FIG. 5: Two orthogonal Latin squares of order three, also called Graeco-Latin square, can be visualized with a set of nine cards, labeled from 1 to 9.

Orthogonality of both squares implies that all pairs of symbols (nine cards in the figure) are different. Thus the pattern shown in Fig. 5 can be encoded by the permutation matrix P_9 of order 9. It determines which card, ordered in a way natural for bridge players, $\{A\spadesuit, A\diamond, A\clubsuit, K\spadesuit, K\diamond, \dots, Q\clubsuit\}$, should be placed in

which position of the square, labeled in the bottom line,

$$P_9 = \begin{pmatrix} \begin{array}{ccc|ccc|ccc} \text{A}\heartsuit & 0 & 0 & 0 & 0 & 0 & 0 & 0 & 0 \\ 0 & 0 & 0 & 0 & 0 & 0 & 0 & \text{A}\diamond & 0 \\ 0 & 0 & 0 & 0 & 0 & \text{A}\clubsuit & 0 & 0 & 0 \\ \hline 0 & 0 & 0 & 0 & 0 & 0 & 0 & 0 & \text{K}\spadesuit \\ 0 & 0 & 0 & \text{K}\diamond & 0 & 0 & 0 & 0 & 0 \\ 0 & \text{K}\clubsuit & 0 & 0 & 0 & 0 & 0 & 0 & 0 \\ \hline 0 & 0 & 0 & 0 & \text{Q}\spadesuit & 0 & 0 & 0 & 0 \\ 0 & 0 & \text{Q}\diamond & 0 & 0 & 0 & 0 & 0 & 0 \\ 0 & 0 & 0 & 0 & 0 & 0 & \text{Q}\clubsuit & 0 & 0 \end{array} \end{pmatrix}, \quad (11)$$

where each card represents the number 1. To assure that each rank and each suit of cards do not repeat in each row and column of the square the non-zero entries of the matrix P_9 satisfy the rules of a strong Sudoku: in each row, column and block there is a single non-zero entry. Moreover, all the locations of these entries in each block are different. Alternatively, the design can be described by a table of size 9×4 , in which for each card we write four digits: the value ‘v’ (or rank of a card), its suit ‘s’, the row ‘r’ and the column ‘c’ in the square, each running from 1 to 3. Conditions of OLS imply that there exist three *invertible* functions, which map a pair of two digits into the other two, $(v, s) = F_1(r, c)$; $(v, r) = F_2(s, c)$ and $(v, c) = F_3(s, r)$.

In other words, the permutation matrix P_9 is two-unitary, and restructured into $T_{ij,kl}$ forms a perfect tensor with four indices running from 1 to 3, so that the partially transposed matrix P_9^T and the reshuffled matrix P_9^R also form permutations, and are thus unitary and invertible. Making use of the coding: (A; K; Q) \leftrightarrow (1; 2; 3) and (\heartsuit ; \diamond ; \clubsuit) \leftrightarrow (1; 2; 3) one can represent the Graeco-Latin square in the numeric form,

$$\begin{array}{|c|c|c|} \hline 11 & 23 & 32 \\ \hline 22 & 31 & 13 \\ \hline 33 & 12 & 21 \\ \hline \end{array} \quad (12)$$

To see a direct relation to quantum entanglement observe that the above design allows us to construct the state AME(4, 3) appearing in Eq. (9): each of the nine terms of the four-partite state corresponds to a single card, two first digits are given by its position in the square (row and column), the third one is determined by its rank and the fourth by the suit. As this construction works for an OLS of an arbitrary dimension, we conclude that the states AME(4, d) exist for all these dimensions, for which OLS(d) are known. It is easy to construct such a design if d is a prime or a power of a prime. Furthermore, OLS are known to exist for any $d \geq 7$ [15]. However, such a configuration does not exist for $d = 6 = 2 \times 3$, as conjectured by Euler, who formulated his famous problem of 36

officers, coming from six different units, of six ranks in each unit. This fact was proved in 1900 by Tarry [17, 18]. To put some light on Euler’s problem we invite the reader to study a particular attempt to solve it, shown in Fig. 6.

A♥	K♠	Q♣	J♦	10♠	9♠
9♣	10♦	K♠	A♠	Q♠	J♥
K♠	A♠	?	?	9♦	10♣
J♠	Q♠	?	?	A♣	K♦
10♠	9♥	A♦	K♣	J♠	Q♠
Q♦	J♣	10♠	9♠	K♥	A♠

FIG. 6: To find a solution of the Euler problem of 36 officers one needs to place four missing cards into the center of the square, in such a way that neither the ranks of the cards nor their suits are repeated in each row and each column.

As there is no solution of the original problem of Euler, there are no 2-unitary permutation matrices of size 36. However, one can relax the assumption that we look for a permutation matrix of order 36 and look for a solution in the larger continuous group of unitary matrices $U(36)$. This step is equivalent to leaving the well studied ground of classical combinatorial designs, and moving to a more general class of their quantum analogues.

VI. QUANTUM ORTHOGONAL LATIN SQUARES

As a known rule of thumb, every good notion can be quantized. A cornerstone of the flourishing new field of *quantum combinatorics* was laid by Gerhard Zauner, who introduced quantum analogues of classical designs in his Ph.D Thesis from 1999 [52]. A quantum combinatorial design consists of quantum states from a complex Hilbert space \mathcal{H}_d , arranged with a certain ‘symmetry and balance’.

Such an approach to the classical notion of Latin squares was first advocated by Musto and Vicary [53], who proposed to replace classical symbols in the square by pure quantum states. They defined a *quantum Latin square* (QLS) of size d , which consists of d^2 quantum states $|\psi_{ij}\rangle \in \mathcal{H}_d$, with $i, j = 1, \dots, d$, such that each column and each row of the square form an orthogonal basis. The classical condition: all objects in each row and each column are *different*, is replaced here by its natural quantum analog: all quantum states in each row and

column are *orthogonal*.

$ 1\rangle$	$ 2\rangle$	$ 3\rangle+ 4\rangle$	$ 3\rangle- 4\rangle$
$ 3\rangle$	$ 4\rangle$	$ 1\rangle- 2\rangle$	$ 1\rangle+ 2\rangle$
$ 2\rangle+ 4\rangle$	$ 1\rangle- 3\rangle$	$ 1\rangle+ 2\rangle+ 3\rangle- 4\rangle$	$ 1\rangle- 2\rangle+ 3\rangle+ 4\rangle$
$ 2\rangle- 4\rangle$	$ 1\rangle+ 3\rangle$	$ 1\rangle+ 2\rangle- 3\rangle+ 4\rangle$	$ 1\rangle- 2\rangle- 3\rangle- 4\rangle$

FIG. 7: Quantum Latin square of order $d = 4$, which consists of 16 different states – normalization constants are omitted. Each of its rows and columns forms an orthogonal basis in \mathcal{H}_4 , as required. This design satisfies also a stronger condition of a quantum sudoku, as four states in each 2×2 block also form an orthogonal basis.

An example of a quantum Latin square shown in Fig. 7, borrowed from [54], satisfies also rules of a *quantum sudoku* [55]: each row, column and block form an orthogonal basis. Note that any classical Latin square (or a classical sudoku pattern) can be ‘quantized’ in a trivial way, by placing each symbol inside a ket and treating it as a quantum state $|\psi\rangle$. In such a case the design contains d copies of d different states which form several copies of the standard computational basis. On the other hand, the quantum design shown in Fig. 7 consists of 16 different states $|\psi_{ij}\rangle$, which form together 12 different orthogonal bases. Replacing each state $|\psi_{ij}\rangle$ in field (i, j) of the square by the projector $|\psi_{ij}\rangle\langle\psi_{ij}|$ one obtains a *blockwise bistochastic* matrix: positive operators in each row and each column sum to identity. Such designs were recently analyzed in [56, 57] under the name *quantum magic squares*. The design presented in Fig. 7 certainly deserves such a name, as all its entries are different, just as in the classical case.

To look for a broader class of quantum AME states one has to consider quantum analogues of two orthogonal Latin squares. The first attempt to construct such a quantum pattern [58], was later improved in [59], but we follow here the version used in [21, 22]. Before presenting a definition of such a quantum combinatorial design, let us list the rules of Euler defining a classical OLS(d), which consists of d^2 symbols, each described by its color and rank:

C1) all d^2 symbols are different,

C2) all d symbols in each row are of different colors and different ranks,

C3) all d symbols in each column are of different colors and different ranks.

This list will be helpful to understand the corresponding quantum constraints.

Definition. A pair of quantum orthogonal Latin squares (QOLS) of size d is defined as a set of d^2 bi-

partite states, $|\psi_{ij}\rangle \in \mathcal{H}_A \otimes \mathcal{H}_B$ which form a square,

$$\text{QOLS} := \begin{bmatrix} |\psi_{11}\rangle & \dots & |\psi_{1d}\rangle \\ \dots & \dots & \dots \\ |\psi_{d1}\rangle & \dots & |\psi_{dd}\rangle \end{bmatrix}, \quad (13)$$

and satisfy constraints **Q1)–Q3)** specified below, analogous to the classical conditions **C1)–C3)**.

There is a natural way to quantize condition **C1)**, imposing that all the objects of the classical design are different:

Q1) All d^2 states in the pattern are mutually orthogonal and they form a basis in $\mathcal{H}_d \otimes \mathcal{H}_d$,

$$\langle\psi_{ij}|\psi_{k\ell}\rangle = \delta_{ik}\delta_{j\ell}. \quad (14)$$

The classical conditions **C2)–C3)** require some explanation. In each row (or column) we analyze separately colors (or ranks) of the symbols in the classical pattern. Thus one can expect that the analogous quantum constraints concern the partial traces of symmetric combinations of projectors. As in the classical design no color is repeated in each row and column the ‘average color’ should be ‘white’. Therefore, in quantum designs, it is assumed [61] that the partial trace over the second subsystem B (or the first subsystem A) is maximally mixed and there are no correlations between different rows (and different columns).

Q2) All rows of the square satisfy the partial trace conditions

$$\sum_{k=1}^d \text{Tr}_B(|\psi_{ik}\rangle\langle\psi_{jk}|) = \delta_{ij}\mathbb{I}_d. \quad (15)$$

Dual conditions hold for the other partial trace Tr_A , analogous to the requirement that all ranks in each row of the classical design are different.

Q3) All columns of the square satisfy analogous conditions

$$\sum_{k=1}^d \text{Tr}_B(|\psi_{ki}\rangle\langle\psi_{kj}|) = \delta_{ij}\mathbb{I}_d, \quad (16)$$

and dual conditions for Tr_A .

Observe that the above conditions are satisfied by any classical design, upgraded to a quantum setup by replacing any symbol by the corresponding product state, e.g. $A\spadesuit \rightarrow |A\spadesuit\rangle = |11\rangle \in \mathcal{H}_d \otimes \mathcal{H}_d$. Since conditions **Q1)–Q3)** are invariant with respect to local unitary operations, $U_A \otimes U_B$, with $U_A, U_B \in U(d)$, they are also satisfied by orthogonal apparently quantum Latin squares, obtained from any classical solution by a local unitary transformation. However, a legitimate quantum solution can contain also entangled states $|\psi_{ij}\rangle$, for instance a Bell

state, $|\mathbf{A}\spadesuit\rangle + |\mathbf{K}\heartsuit\rangle$, also written as $|11\rangle + |22\rangle$, so in general it is not possible to split a pair of QOLS into two separate classical designs OLS.

Note that the above three requirements ensure that the state generated from the collection of d^2 bipartite states, $\{|\psi_{ij}\rangle\}_{i,j=1}^d$ forming a QOLS,

$$|\Psi_{ABCD}\rangle = \frac{1}{d} \sum_{i,j=1}^d |i\rangle_A |j\rangle_B |\psi_{ij}\rangle_{CD}, \quad (17)$$

is an AME(4, d) state [22]. To show this let us combine indices (i, j) into a composite index $\mu = 1 \dots d^2$ and merge the vectors $|\psi_\mu\rangle$ into a matrix $U_{\mu,\nu}$, where the other composite index, $\nu \leftrightarrow (k, \ell)$, labels d^2 components of each vector $|\psi_\mu\rangle$. Then the quantum conditions **Q1**-**Q3**, related to the maximal entanglement for three different splittings of the system $ABCD$, imply that the matrix $U_{\mu,\nu}$ is 2-unitary, or equivalently, the corresponding tensor T_{ijkl} is perfect, as necessary and sufficient to generate a four-party AME state [14].

In this way we arrived at the following statement [21, 61].

Observation 1. *Existence of a state $|\text{AME}(4, d)\rangle \in \mathcal{H}_d^{\otimes 4}$ is equivalent to:*

- E1) existence of QOLS(d);
- E2) existence of a 2-unitary matrix $U \in U(d^2)$;
- E3) existence of a perfect tensor T_{ijkl} with four indices, each running from 1 to d .

A perfect tensor T reshaped into rows, $i, j, |\psi_{ij}\rangle$ forms a quantum orthogonal array (QOA) with 4 columns, d^2 rows of strength $k = 2$ and alphabet containing of d symbols [58]. The array can be divided into two classical columns i, j , and two quantum columns, containing possibly entangled states $|\psi_{ij}\rangle$, so it is written QOA($d^2, 2_C + 2_Q, d, 2$). An AME state of four subsystems with d levels each leads to a quantum code $((4, 1, 3)_d)$, which allows one to encode one state of a d -level systems in four such systems and correct a single error [60]. Therefore, Observation 1 concerning equivalence relations can be extended by the following two items:

- E4) existence of a quantum orthogonal array of strength $k = 2$ with d^2 rows, 4 columns and d -letters symbols, denoted as QOA($d^2, 2_C + 2_Q, d, 2$).
- E5) existence of a four-qudit quantum code $((4, 1, 3)_d)$.

Before discussing the Euler's case $d = 6$ let us return to the simpler case of $d = 2$, for which there are no Graeco-Latin squares. As discussed in [23] even using two-qubit entangled states it is not possible to construct a QOLS of order two, in accordance to the result of Higuchi and Sudbery, who demonstrated that there are no AME states for a four-qubit system [11].

VII. SOLUTION OF THE QUANTUM EULER PROBLEM FOR $d = 6$ AND ITS GEOMETRIC CONSEQUENCES

The problem whether there exist quantum orthogonal Latin squares of order six, or equivalently, AME state of four subsystems with six levels each, was studied for a few recent years [21, 58, 62], but the solution was found only recently [22]. We looked for a 2-unitary matrix $U \in U(36)$, such that its partial trace U^Γ and reshuffling U^R , are also unitary, so that its rows (or columns) treated as pure states of a 6×6 system determine the solution $\{|\psi_{ij}\rangle\}_{i,j=1}^d$.

This task was performed numerically by the following iterative procedure. For any initial matrix X_0 of size 36 we take the corresponding unitary V obtained by its polar decomposition, $X_0 = HV$, then write its reshuffling in the similar form, $X' = V^R = H'W$ with a unitary W . The output matrix X_1 is then obtained by partial transpose of the resulting unitary, $X_1 = W^\Gamma$. Repeating such a Sinkhorn-like algorithm [63] several times one generates a sequence of matrices X_n , but its convergence to a 2-unitary matrix is not guaranteed. As the search is performed in the huge space $SU(36)$ of 1295 real dimensions, the results depend critically on the choice of the seed X_0 .

By inserting four cards missing in Fig. 6 we obtain an approximation of the non-existing classical pattern OLS(6) and generate a certain permutation matrix P_{36} , which determines which card goes into which field of the square. Such a matrix, maximizing the entangling power among all bi-partite permutations [64], if perturbed by a small random perturbation Y , gives a seed of the type $X_0 = P_{36} + \epsilon Y$. Such an initial point generates a trajectory X_n , typically converging (at $n \sim 400$) to a matrix U_{36} , two-unitary up to the numerical accuracy [22]. Making use of the freedom of local unitary transformations it was possible to find a product basis, in which U_{36} becomes sparse [65, 66], and to bring it to the block diagonal form.

Imposing unitarity in each of its nine blocks of size four one could derive a fully analytical solution of the problem. The resulting 2-unitary matrix U_{36} has 112 non-zero entries, not more than four in each row. All entries share one of three possible amplitudes, $a = \frac{1}{2}\sqrt{1 - 1/\sqrt{5}}$, $b = \frac{1}{2}\sqrt{1 + 1/\sqrt{5}}$, and the largest one, $c = 1/\sqrt{2}$. Interestingly, the ratio of the two smaller numbers gives the golden mean, $\varphi = b/a = (1 + \sqrt{5})/2$, so the pattern was called a *golden AME state* [22]. The solution is visualized in Fig. 8 by 112 cards of six suits and six ranks, placed in the square of size 6, so that each field represents a single state $|\psi_{ij}\rangle$ forming the QOLS(6). There are no more than 4 cards in each field and the size of each symbol represents its amplitude. Complex phases of each entry, being multiples of $\omega = \exp(i\pi/10)$, are provided in [22].

Observe that 36 cards can be divided into nine groups of four cards of the same colour and neighbouring ranks,

K♠	A♦	<u>10♠</u> 10*	<u>10♠</u> 10♣	Q♦ Q♥	Q♣ Q*
A♣	K♥	9♣ 9*	9♣ 9♣	J♦ J♥	J♣ J*
9♠	10♦	Q♣ Q*	Q♠	A♦ A♥	A♣ A*
10♣	9♥	J♣ J*	J♣	K♦ K♥	K♣ K*
Q♣	J♠	K♦	A♣ A*	10♠	<u>10♦</u> 10♥
J*	Q♣	A♥	K♣ K*	9♣	9♦ 9♥
A♣ A*	A♠ A♣	<u>10♦</u> 10♥	<u>10♠</u> 10*	Q♣ Q♥	Q♦ Q♥
K♣ K*	K♠ K♣	9♦ 9♥	9♣ 9*	J♠ J♥	J♦ J♥
9♦	9♣	Q♠ Q♥	Q♦	A♣ A*	A♠
10♥	10*	J♠ J♥	J♥	K♣ K*	K♣
J♦	J*	A♠ A♣	A♦ A♥	10♣	10♠ 10♣
Q♥	Q♣	K♠ K♣	K♦ K♥	9*	9♠ 9♣

FIG. 8: Solution of the quantum version of the Euler problem constructed in [22]: several cards in a single field represent an entangled state, say a Bell state, $|\psi_{11}\rangle = |\mathbf{K}\spadesuit\rangle + |\mathbf{A}\clubsuit\rangle$, or in a usual notation, $|11\rangle + |22\rangle$, in the upper left corner. The size of each card encodes the amplitude in the superposition: large c (large symbol), medium b (smaller symbol), and the smallest a (underlined symbol), while analytically known complex phases are listed in the original work. This solution was called *golden*, as the ratio b/a gives the golden mean.

so that all entries of the quantum design, represented by cards in a single cell of the square, contain superpositions of the cards from a single group. Looking at Fig. 8 it is easy to realize that the average suits and ranks in each column and each row of the square are balanced. However, to verify that all the necessary conditions **Q1)**-**Q3)** are indeed satisfied one needs to use the complex phases found, as explicitly shown in Ref. [23].

We shall now analyze certain geometric consequence of the established solution of the quantum version of the problem of Euler. Consider, in general, an $N = 4$ party system $ABCD$ with local dimension d . The known fact that for $d = 2$ there are no AME states [11], implies the following statement concerning the manifolds of maximally entangled states $\mathcal{P}_{\max} = PU(4) = U(4)/U(1)$ of the 4×4 bi-partite system determined by three symmetric splittings of $ABCD$.

Observation 2. *Non-existence of the state $|\text{AME}(4,2)\rangle \in \mathcal{H}_2^{\otimes 4}$ implies that the following intersection of three projective group manifolds, corresponding to various splittings, all embedded in $\mathbb{C}P^{15}$, is empty,*

$$PU(4)_{CD}^{AB} \cap PU(4)_{BD}^{AC} \cap PU(4)_{BC}^{AD} = \emptyset. \quad (18)$$

Let us emphasize at this point that conjecture d) formulated in Section III concerning non-displaceability of

the projective group manifold $PU(4)$ in $\mathbb{C}P^{15}$ implies that two copies of this manifold do intersect, but this does not imply that three copies will meet in a single point. Unitary matrices $U \in U(d^2)$ with the property that the reshuffled matrix is unitary, $U^R \in U(d^2)$, are called *dual unitary* [67, 68]. It comes then not as a great surprise that dual unitary matrices exist for any dimension [69, 70], what is directly implied by the non-displaceability conjecture. The same statement holds for unitary matrices, for which partial transpose is unitary $U^\Gamma \in U(d^2)$, analyzed earlier in [71].

In some analogy to properties of physical systems containing interacting spins, the non-existence of AME states for a four-qubit system was dubbed *frustration* [9], as the requirement of maximal entanglement with respect to two given splittings contradicts an analogous condition for the third splitting. As the number of constraints for an AME state is so big, that they can not be simultaneously fulfilled for $d = 2$, the frustration disappears in higher dimensions.

The case $d = 6$ was particularly interesting, as the lack of solution of the classical Euler problem of 36 officers did not allow one to generate the corresponding four-quhex entangled state. The explicit analytic solution of the quantum version of the problem constructed in [22] has also a geometric interpretation.

Observation 3. *Existence of the state $|\text{AME}(4,6)\rangle \in \mathcal{H}_6^{\otimes 4}$ implies that the intersection of the following three manifolds embedded in $\mathbb{C}P^{36^2-1}$ is non-empty,*

$$PU(36)_{CD}^{AB} \cap PU(36)_{BD}^{AC} \cap PU(36)_{BC}^{AD} \supset \{\text{AME}(4,6)\}. \quad (19)$$

It is rather difficult to imagine how these high-dimensional manifolds embedded in a complex projective space do intersect. Thus, in Fig. 9 we use the standard sphere S^2 to present a simple caricature of this property.

VIII. CONCLUDING REMARKS

The recent construction of an AME state of four subsystems with six levels each presented in [22] and further analyzed in [23] closes the last gap at $d = 6$ and implies that $\text{AME}(4, d)$ states exist for any dimension $d \geq 3$. As explained in Observation 1, the explicit construction of the state $\text{AME}(4, 6)$ implies that there exist:

- 1) a solution QOLS(6) to the quantum version of the problem of Euler,
- 2) a 2-unitary matrix $U_{36} \in U(36)$,
- 3) a perfect tensor [50] T_{ijkl} with four indices, each running from 1 to 6,
- 4) a quantum orthogonal array [58] with $r = 36$ rows, $N_C = 2$ classical columns and $N_Q = 2$ quantum, and $d = 6$ -letters symbols of strength $k = 2$, written $\text{QOA}(36, 2_C + 2_Q, 6, 2)$,
- 5) a quantum code $((4, 1, 3))_6$ which allows one to encode one quhex in four such systems – see [60].

Note that the existence of the golden $|\text{AME}(4, 6)\rangle$ state corresponding to the problem of 36 *quantum officers* of Euler has some direct applications in processing of quantum information [10]. Consider a set of four dice, each with six faces, prepared in such a maximally entangled state. Any pair of dice is unbiased, although performing measurements on any selected pair of dice one can predict the outcome of the measurement done on the other two. A similar protocol cannot work with four coins, as there are no AME states for four-qubit system.

The results mentioned above have also direct geometric implications. Results presented in [11] imply that there are no absolutely maximally entangled states of a four qubit system $ABCD$. Thus, three copies of the projective group manifold $PU(4)$, each consisting of pure states maximally entangled with respect to three different splittings, embedded in $\mathbb{C}P^{15}$ do not intersect in a single point [11]. However, for any dimension $d \geq 3$ such four-party entangled states do exist. Therefore, if $d \geq 3$ then three copies of the manifold $PU(d^2)$, corresponding to three different splittings of the four-qudit system $ABCD$, mutually intersect. This non-empty set of intersection consists of 2-unitary matrices from $U(d^2)$.

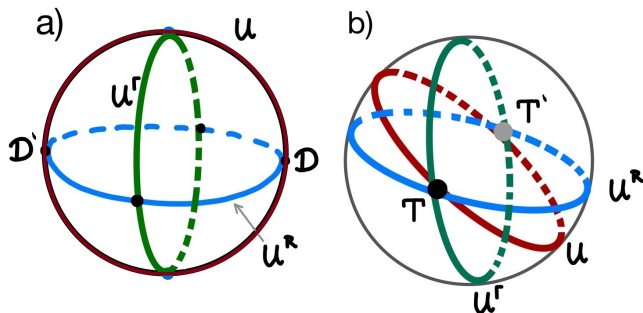


FIG. 9: Intersection of manifolds \mathcal{P}_{\max} of maximally entangled states. a) $d = 2$: manifold of maximally entangled states of two ququarts, corresponding to the projective unitary group $PU(4)$, embedded in $\mathcal{P}_{16} = \mathbb{C}P^{15}$, is represented by a great circle on the sphere. Such three circles, each representing matrices such that U or U^R or U^T are unitary, do not meet in a single point, as there are no 2-unitary matrices in $U(4)$. Since the manifold $\mathcal{P}_{\max} = U(4)/U(1)$ is conjectured to be non-displaceable, its two copies do intersect: point D represents dual unitary matrices; b) $d \geq 3$: three copies of the manifold \mathcal{P}_{\max} , representing three different splittings of $ABCD$, do intersect at a point corresponding to a two-unitary matrix T in $U(d^2)$.

It is not simple to visualize mutual intersections of such highly dimensional manifolds. Hence, in Fig. 9 each projective group manifold $PU(d^2)$ is represented by a great circle S^1 on a sphere S^2 . In the case $d = 2$ three such manifolds (great circles) do not mutually intersect – see Fig. 9a. Lack of the AME states for four-qubit systems can be related to *frustration* [72, 73]: Requiring that certain two conditions hold, say matrices U and U^R

are unitary, implies that the third condition, $U^T \in U(4)$, cannot be satisfied. In a geometric perspective, if a point belongs to the intersection of two circles, it cannot belong to the third one. Fortunately frustration can be lifted if the number of degrees of freedom increases. This is the case if one studies the same $\text{AME}(4, d)$ problem for any $d \geq 3$. Then there exist a 2-unitary matrix $U \in U(d^2)$ such that U^T and U^R are unitary, so that three circles meet in a single point – see Fig. 9b).

It is easy to guess that such a simplistic visualization cannot display correctly all the features of multidimensional manifolds. For instance, the set D of dual unitary matrices [67, 68] formed by cross-section of two manifolds, corresponding to U and U^R being unitary, does not consist of discrete points only, but forms a continuous set [69, 74]. As dual unitary matrices maximize the distance to the local product gates [75], in the space of bi-partite unitary gates they play the role of the maximally entangled states in the space of bi-partite pure quantum states. Furthermore, the fact that three circles plotted in Fig. 9b) intersect at the two-unitary matrix T and also at the antipodal point T' has no relation to the open problem concerning the classification of AME states of a N subsystems with d levels each, which are not locally equivalent [76, 77].

Let us emphasize that no real solution for the AME states of four subsystems with six levels each was found. It was then conjectured [22] that no real 2-unitary orthogonal matrices of size 36 exist. From a geometric perspective it is thus interesting to analyze differences between the structures of various manifolds embedded in the complex and in the real projective spaces. Frustration can also be relaxed if instead of considering standard quantum states one replaces complex coefficients, by vectors with $n_c > 2$ real numbers [78].

Note also that mutually orthogonal Latin cubes correspond to six-party states $|\text{AME}(6, d)\rangle$ and 3-unitary matrices of size d^3 , while M -dimensional Latin hypercubes determine AME states of $N = 2M$ subsystems and M -unitary matrices of order d^M , with the property that all their reorderings remain unitary [14]. It is clear that known combinatorial results concerning the existence of such orthogonal Latin cubes and hypercubes [12], implies existence of certain multipartite entangled states and can also be translated into the geometric language of intersection of the corresponding projective groups embedded in the complex projective space.

It is a pleasure to thank S. A. Rather, A. Burchardt, W. Bruzda, G. Rajchel-Mieldzioc and A. Lakshminarayan for a long and fruitful collaboration on the quantum version of the problem of Euler and to Z. Puchała and L. Rudnicki for mutual research on mutually maximally entangled states. The author is grateful to P. Kielanowski for the invitation to a conference in Białystok, during which this work was presented, and for an effective encouragement to complete this paper. Furthermore, I am obliged to J. Buczyński for organizing in Warsaw a successful workshop *Tensors from physics*

view point, during which the final scope of this contribution was reshaped in discussions with A. Borówka and A. Sawicki. I am thankful to W. Bruzda for preparing Figs. 6 and 8, to M. Życzkowska for drawing the other figures and to I. Bentgsson, M. Grassl, R. Horodecki and S. Pascazio for numerous remarks on the manuscript. This work was supported by Narodowe Centrum Nauki under the Quanterra project number 2021/03/Y/ST2/00193 and by Foundation for Polish Science under the Team-Net project no. POIR.04.04.00-00-17C1/18-00.

Appendix A: Glossary of key mathematical terms used

1. Algebraic

Consider a matrix A of order d with entries $A_{ij} = \langle i|X|j\rangle$. According to the standard notation A^T represents the **transposed** matrix with entries A_{ji} , while A^\dagger denotes the Hermitian conjugate, $A_{ij}^\dagger = A_{ji}$. A matrix U is called *unitary* if $UU^\dagger = \mathbb{I}_d$.

It is convenient to describe a bi-parite $d \times d$ state in a composed Hilbert space $\mathcal{H}_d \otimes \mathcal{H}_d$. Introducing a product basis $|a, i\rangle = |a\rangle \otimes |i\rangle$, one can represent entries of a matrix X of size d^2 in a 4-index notation $X_{\substack{ai \\ bj}} = \langle a, i|X|b, j\rangle$ – see [51]. Then the **transposed** matrix reads, $(X_{\substack{ai \\ bj}})^T = X_{\substack{bj \\ ai}}$.

A1. Partial transpose is obtained by action of the transpose on a single subsystem only. Partially transposed matrix X^Γ consist of entries transposed in each block, $(X_{\substack{ai \\ bj}})^\Gamma = X_{\substack{aj \\ bi}}$, so that the second pair of indices is exchanged. There exist dual operation of partial transpose with respect to the first subsystem, $(X_{\substack{ai \\ bj}})^\Gamma = X_{\substack{bi \\ aj}}$, and their concatenation produces the standard transpose, $(X^\Gamma)^\Gamma = (X^\Gamma)^\Gamma = X^T$.

A2. Reshuffling X^R of a matrix X of size d^2 , (also called *reordering*), consists in reshaping rows of a matrix of length d^2 into square blocks of size d . This corresponds to a diagonal swap of the indices, $(X_{\substack{ai \\ bj}})^R = X_{\substack{ab \\ ij}}$, and the dual transformation producing $X_{\substack{ji \\ ba}}$ has similar properties [51].

A3. Dual unitary matrix X of size d^2 satisfies two conditions: a) it is unitary, $X \in U(d^2)$, and b) its reshuffling is also unitary, $X^R \in U(d^2)$ – see [63, 67]. Such matrices are represented in Fig. 9a by the intersection of two circles.

A4. Two-unitary matrix X of size d^2 , introduced earlier in [14], satisfies *three* conditions: a) $X \in U(d^2)$, b) $X^R \in U(d^2)$, c) $X^\Gamma \in U(d^2)$. Thus this property is stronger as the previous one and any 2-unitary U is also dual-unitary. Two-unitary matrices correspond in Fig. 9b to the intersection of three circles. An example of a 2-unitary permutation matrix P_9 of order nine is obtained

by replacing each card in Eq. (11) by digit 1.

A5. Multi-unitary matrix X of size d^M , labeled by $2M$ indices, is unitary, $X \in U(d^M)$, and it remains unitary under reordering of its entries corresponding to an arbitrary symmetric partition of $2M$ indices [14]. The number of such partitions is $\binom{2M}{M}$. Since we know that if U is unitary so is U^T , the number of conditions to be checked to establish M -unitarity is thus $\frac{1}{2} \binom{2M}{M}$, which gives 3 conditions for 2-unitarity and 10 conditions for 3-unitarity.

A6. Flattening of a tensor with more than two indices denotes its reshaping into a matrix. A tensor T_{ijkl} , with four indices, each running from 1 to d , can be transformed into a matrix in three ways, corresponding to projections of this hypercube into three different planes. Defining two composite indices, $\mu = (i-1)d + j$ and $\nu = (k-1)d + \ell$, we can represent the tensor as a matrix of size d^2 with entries $X_{\mu\nu} = T_{ij,k\ell}$. If the index μ is composed by the pair (i, k) one obtains another flattening, $Y_{\mu\nu} = T_{ik,j\ell}$, while the third choice, (i, ℓ) , leads to the matrix $Z_{\mu\nu} = T_{i\ell,kj}$. All three flattenings are related by the reorderings defined above, as $Y = X^R$ and $Z = X^\Gamma$.

A7. Perfect tensor has the property that all its flattenings are unitary up to a constant [50]. Hence a four-index tensor T_{ijkl} restructured into a matrix gives a 2-unitary matrix e.g. $X_{\mu\nu} = T_{ij,k\ell}$, such that all its reorderings remain unitary.

2. Combinatorial

B1. Latin square of order d , written as LS(d), consists of d copies of d symbols, arranged into a square such that each row and each column contains different symbols. These configurations exist for any dimension d [12].

B2. Graeco-Latin square of order d , also called a pair of *orthogonal Latin squares*, written OLS(d), are formed by two Latin squares which are *orthogonal*. This means that all d^2 pairs of symbols placed in each cell of the square are different – see conditions C1)– C3) in Sec. VI. These configurations exist [12] for $d = 3, 4, 5$ and $d \geq 7$. A collection of m LS of order d is called mutually orthogonal Latin squares, denoted as m -MOLS(d), if any two of them are orthogonal. There exist not more than $(d-1)$ MOLS(d) and this bound is saturated for dimension d being a prime or a power of prime [15].

B3. Latin cube of order d , written as LC(d), consists of d^2 copies of d symbols, arranged into a cube such that each row, each column and each line contain each of the symbols exactly once. In analogy to OLS one defines also orthogonal Latin cubes and orthogonal Latin hypercubes of an arbitrary dimension n [79]. Latin cubes are used in coding theory.

B4. Orthogonal array with r runs, N factors, d levels and strength k , written $\text{OA}(r, N, d, k)$, forms a rectangular $r \times N$ table with entries coming from a d -letter alphabet arranged in such a way that in every collection of k columns each of the possible ordered pairs of elements appears the same number of times [80]. Observe that $\text{LS}(d)$ is equivalent to $\text{OA}(d^2, 3, d, 2)$, while $\text{LC}(d)$ to $\text{OA}(d^3, 4, d, 3)$. In general, $\text{OA}(d^2, 2 + m, d, 2)$ defines a set of m -MOLS(d).

B5. Quantum Latin square of order d , written $\text{QLS}(d)$, is a collection of d^2 quantum states, $|\psi_{ij}\rangle \in \mathcal{H}_d$, arranged into a square such that in each row and each column all states are orthogonal and form an orthogonal basis [53]. If the number of different states in the design exceeds d then the design is genuinely quantum [54], as it cannot be transformed into a classical LS by a unitary rotation.

B6. Quantum orthogonal Latin squares of order d , written $\text{QOLS}(d)$, is a collection of d^2 bi-partite quantum states $|\psi_{ij}\rangle \in \mathcal{H}_d \otimes \mathcal{H}_d$ arranged into a square of size d such that conditions Q1)–Q3) listed in Sec. VI are satisfied [21]. Such designs exist for any $d \geq 3$ [22].

B7. Quantum orthogonal array $\text{QOA}(r, N = N_C + N_Q, d, k)$ is an arrangement consisting of r rows composed of N -partite quantum states with d levels each, $|\phi_j\rangle \in \mathcal{H}_d^{\otimes N}$, such that for any subset \mathcal{I} consisting of $(N - k)$ subsystems the following partial trace relation holds [58], $\sum_{j=1}^N \text{Tr}_{\mathcal{I}}(|\phi_j\rangle\langle\phi_j|) \propto \mathbb{I}_{d^k}$. Out of N columns of the entire design one distinguishes a certain number N_C of classical columns containing product states and the remaining $N_Q = N - N_C$ quantum columns consisting of entangled states. Classical OA correspond to the case $N_C = N$ and $N_Q = 0$. The notion of QOA forms a natural generalization of other quantum designs. For instance, $\text{QOA}(8, 3_C + 3_Q, 2, 3)$ is equivalent to $3\text{QOLC}(2)$, which corresponds to the state $\text{AME}(6, 2) \in \mathcal{H}_2^{\otimes 6}$ [58], while $\text{QOA}(36, 2_C + 2_Q, 6, 2)$ gives $2\text{QOLS}(6)$ and the state $\text{AME}(4, 6) \in \mathcal{H}_6^{\otimes 4}$ [22].

3. Geometric

G1. Manifold \mathcal{M} is a topological space locally equivalent to Euclidean space. Examples include circle, sphere, and projective space. These examples form

closed, compact and connected n -manifolds of a fixed dimension n .

G2. Real projective space $\mathbb{R}P^n$ – a compact, smooth manifold of dimension n defined as a space of lines passing through the origin in \mathbb{R}^{n+1} . Examples include $\mathbb{R}P^1$ topologically equivalent to the circle S^1 , $\mathbb{R}P^2$, called real projective plane, which can be obtained from the sphere S^2 by identifying antipodal points and $\mathbb{R}P^3$, diffeomorphic to $SO(3)$ and $U(2)/U(1)$.

G3. Complex projective space $\mathbb{C}P^n$ is the projective space with respect to the field of complex numbers. It forms a complex, compact, smooth manifold of $2n$ real dimension and can be regarded as a quotient space, $\mathbb{C}P^n = S^{2n+1}/U(1)$ so that $\mathbb{C}P^1 = S^3/S^1 = S^2$.

G4. Symplectic manifold is a smooth manifold \mathcal{M} , equipped with a closed nondegenerate differential 2-form ω , called the symplectic form. Symplectic manifold is used in classical mechanics to represent the phase space.

G5. Lagrangian manifold \mathcal{L}_n of dimension n is a differentiable submanifold of a $2n$ -dimensional symplectic manifold \mathcal{M}_{2n} such that the exterior form ω specifying the symplectic structure vanishes identically on \mathcal{L}_n .

G6. Displaced manifold. An image by a transformation determined by a unitary matrix U of a suitable dimension m of an n -dimensional manifold \mathcal{M} embedded inside \mathcal{N} . A displaced manifold will be written $U\mathcal{M} \subset \mathcal{N}$.

G7. Non-displaceable manifold \mathcal{M} embedded in \mathcal{N} such that \mathcal{M} cannot be displaced unitarily in such a way that it does not intersect its image: For any $U \in U(m)$ one has $\mathcal{M} \cap U\mathcal{M} \neq \emptyset$.

G8. Foliation of an n dimensional manifold \mathcal{M}_n is its decomposition into a union of disjoint leaves – connected submanifolds of dimension p , which can be generated by equivalence classes. The number $q = n - p$, called codimension, determines the dimension of the space of leaves. A foliation is called *singular* if the dimension of the leaves is allowed not to be constant. Singular foliation of $\mathbb{C}P^3$ visualized in Fig. 1 consists of generic leaves of 5 real dimensions, so the codimension q reads $6 - 5 = 1$. In foliation of the 16-dimensional manifold $\mathbb{C}P^8$, presented in Fig. 2, the generic orbit has $p = 14$ real dimensions and its codimension, $q = 16 - 14 = 2$, is equal to the dimension of the triangle of the Schmidt vectors.

[1] A. Peres, *Quantum Theory: Concepts and Methods*, Kluwer Academic, New York, 2002.
[2] B. Mielnik, Geometry of quantum states, *Comm. Math. Phys.* **9**, 55 (1968).
[3] B. Mielnik, Quantum theory without axioms, in *Quantum Gravity II. A Second Oxford Symposium*, edited by C. J. Isham, R. Penrose, and D. W. Sciama, p. 638, Oxford University Press, 1981.
[4] M. A. Nielsen and I. L. Chuang, *Quantum Computation*

and *Quantum Information*, X edition, Cambridge University Press, Cambridge, 2010.
[5] I. Bengtsson, K. Życzkowski, *Geometry of Quantum States. An Introduction to Quantum Entanglement*, II edition, Cambridge University Press, Cambridge 2017.
[6] N. Gisin and H. Bechmann-Pasquinucci, Bell inequality, Bell states and maximally entangled states for n qubits?, *Phys. Lett. A* **246**, 1 (1998).
[7] D. A. Meyer and N. R. Wallach, Global entanglement in

- multipartite systems, *J. Math. Phys.* **43**, 4273 (2002).
- [8] A. J. Scott, Multipartite entanglement, quantum-error-correcting codes, and entangling power of quantum evolutions *Phys. Rev. A* **69**, 052330 (2004).
- [9] P. Facchi, G. Florio, G. Parisi, S. Pascazio, Maximally multipartite entangled states, *Phys. Rev. A* **77**, 060304(R) (2008).
- [10] W. Helwig, W. Cui, J. I. Latorre, A. Riera, and H. K. Lo, Absolute maximal entanglement and quantum secret sharing, *Phys. Rev. A* **86**, 052335 (2012).
- [11] A. Higuchi and A. Sudbery, How entangled can two couples get? *Phys. Lett. A* **272**, 213 (2000).
- [12] C. J. Colbourn, J. H. Dinitz (eds.), *Handbook of Combinatorial Designs*, CRC Press, Boca Raton (2007).
- [13] D. Goyeneche and K. Życzkowski, Genuinely multipartite entangled states and orthogonal arrays. *Phys. Rev. A* **90**, 022316 (2014).
- [14] D. Goyeneche, D. Alsina, J. I. Latorre, A. Riera, and K. Życzkowski, Absolutely Maximally Entangled states, combinatorial designs and multi-unitary matrices, *Phys. Rev. A* **92**, 032316 (2015).
- [15] C. J. Colbourn and J. H. Dinitz, Mutually orthogonal Latin squares: a brief survey of constructions, *J. Stat. Planning Inference* **95**, 9 (2001).
- [16] R. C. Bose, S. S. Shrikhande, E. T. Parker, Further results on the construction of mutually orthogonal Latin Squares and the falsity of Euler's conjecture. *Can. Jour. Math.* **12**, 189–203 (1960).
- [17] G. Tarry, Le problème de 36 officiers, *Compte Rendu de l'Association Francaise pour l'Avancement des Sciences* **1**, 122 (1900).
- [18] D. R. Stinson, A short proof of the nonexistence of a pair of orthogonal Latin squares of order six, *J. Combin. Theory A* **36**, 373 (1984).
- [19] P. Horodecki, L. Rudnicki, K. Życzkowski, Five open problems in quantum information, *PRX Quantum* **3**, 010101 (2022).
- [20] F. Huber, N. Wyderka, *Table of AME states at <http://www.tp.nt.uni-siegen.de/~fhuber/ame.html>*
- [21] A. Rico, *Absolutely maximally entangled states in small system sizes*, Master Thesis, Innsbruck (2020).
- [22] S. A. Rather, A. Burchardt, W. Bruzda, G. Rajchel-Mieldzióć, A. Lakshminarayan, K. Życzkowski, Thirty-six entangled officers of Euler, *Phys. Rev. Lett.* **128**, 080507 (2022)
- [23] K. Życzkowski, W. Bruzda, G. Rajchel-Mieldzióć, A. Burchardt, S. A. Rather, A. Lakshminarayan, $9 \times 4 = 6 \times 6$: Understanding the quantum solution to the Euler's problem of 36 officers, preprint arXiv:2204.06800
- [24] C. F. Dunkl, P. Gawron, J. A. Holbrook, J. Miszczak, Z. Puchała and K. Życzkowski, Numerical shadow and geometry of quantum states, *J. Phys. A* **44** 335301 (19pp) (2011).
- [25] Z. Puchała, J. A. Miszczak, P. Gawron, C. F. Dunkl, J. A. Holbrook, and K. Życzkowski, Restricted numerical shadow and geometry of quantum entanglement, *J. Phys. A* **45**, 415309 (28pp) (2012).
- [26] Ch. Eltschka, M. Huber, S. Morelli, J. Siewert, The shape of higher-dimensional state space: Bloch-ball analog for a qutrit, *Quantum* **5**, 485 (2021).
- [27] Z. Puchała, L. Rudnicki, K. Chabuda, M. Paraniak and K. Życzkowski, Certainty relations, mutual entanglement and non-displaceable manifolds, *Phys. Rev. A* **92**, 032109, (2015).
- [28] C.-H. Cho, Holomorphic discs, spin structures, and Floer cohomology of the Clifford torus, *Int. Math. Res. Not.* **35**, 1803 (2004).
- [29] D. Tamarkin, Microlocal condition for non-displaceability, preprint arXiv:0809.1584 (2008).
- [30] Y.-G. Oh, Floer cohomology of Lagrangian intersections and pseudo-holomorphic discs, *Comm. Pure Appl. Math.* **46**, 995 (1993).
- [31] K. Korzekwa, D. Jennings, T. Rudolph, Operational constraints on state-dependent formulations of quantum error-disturbance, trade-off relations, *Phys. Rev. A* **89**, 052108 (2014).
- [32] O. Andersson, I. Bengtsson, Clifford tori and unbiased vectors, *Rep. Math. Phys.* **79**, 33 (2017).
- [33] L. De Lathauwer, B. De Moor, J. Vandewalle, A multilinear singular value decomposition, *SIAM J. Matrix Anal. Appl.* **21**, 1253 (2000).
- [34] H. A. Carteret, A. Higuchi and A. Sudbery, Multipartite generalisation of the Schmidt decomposition. *J. Math. Phys.* **41** (2000), 7932–7939.
- [35] F. Sokoli and G. Alber, Generalized Schmidt decomposability and its relation to projective norms in multipartite entanglement, *J. Phys. A* **47**, 325301 (2014).
- [36] J.B. Kruskal, Three-way arrays: Rank and uniqueness of trilinear decompositions, with applications to arithmetic complexity, *Lin. Alg. Appl.* **18**, 95 (1977).
- [37] V. Strassen, Rank and optimal computation of generic tensors, *Lin. Alg. Appl.* **52**, 645 (1983).
- [38] J. M. Landsberg, *Tensors: Geometry and Applications* American Mathematical Soc., Providence R.I. (2012).
- [39] V. Vedral and M. B. Plenio, Entanglement measures and purification procedures, *Phys. Rev. A* **57**, 1619 (1998).
- [40] K. Życzkowski, I. Bengtsson, Relativity of pure states entanglement, *Ann. Phys. (N.Y.)* **295**, 115 (2002).
- [41] T.-C. Wei and P. M. Goldbart, Geometric measure of entanglement and applications to bipartite and multipartite quantum states, *Phys. Rev. A* **68**, 042307 (2003).
- [42] S. Tamaryan, T.-C. Wei and D. Park, Maximally entangled three-qubit states via geometric measure of entanglement, *Phys. Rev. A* **80**, 052315 (2009).
- [43] W. Bruzda, S. Friedland, K. Życzkowski, Tensor rank and entanglement of pure quantum states, preprint arXiv:1912.06854
- [44] S. Friedland and L. Wang, Spectral norm of a symmetric tensor and its computation, *Math. Computation* **89**, 2175 (2020).
- [45] S. Friedland and L.-H. Lim, Nuclear Norm of Higher Order Tensors, *Math. Computation* **87**, 1255 (2018).
- [46] P. Facchi, G. Florio, U. Marzolino, G. Parisi and S. Pascazio, Statistical mechanics of multipartite entanglement, *J. Phys. A* **42**, 055304 (2009).
- [47] L. Arnaud and N. Cerf, Exploring pure quantum states with maximally mixed reductions, *Phys. Rev. A* **87**, 012319 (2013).
- [48] F. Huber, O. Gühne, and J. Siewert, Absolutely maximally entangled states of seven qubits do not exist, *Phys. Rev. Lett.* **118**, 200502 (2017).
- [49] F. Huber, C. Eltschka, J. Siewert and O. Gühne, Bounds on absolutely maximally entangled states from shadow inequalities, and the quantum MacWilliams identity, *J. Phys. A* **51**, 175301 (2018).
- [50] F. Pastawski, B. Yoshida, D. Harlow, and J. Preskill,

- Holographic quantum error-correcting codes: Toy models for the bulk/boundary correspondence, *J. High Energy Phys.* **06**, 149 (2015).
- [51] K. Życzkowski and I. Bengtsson, On duality between quantum states and quantum maps, *Open Syst. Inf. Dyn.* **11**, 3 (2004).
- [52] G. Zauner, Quantendesigns – Grundzüge einer nichtkommutativen Designtheorie. Dissertation, Universität Wien, 1999; English translation, *Int. J. Quantum Inf.* **9**, 445 (2004).
- [53] B. Musto and J. Vicary, Quantum Latin squares and unitary error bases, *Quantum Inf. Comput.* **16**, 1318 (2016).
- [54] J. Paczos, M. Wierzbiński, G. Rajchel-Mieldzioc, A. Burchardt, K. Życzkowski, Genuinely quantum SudoQ and its cardinality, *Phys. Rev. A* **104**, 042423 (2021).
- [55] I. Nechita, J. Pillet, SudoQ – a quantum variant of the popular game, *Quantum Inf. Comput.* **21**, 781 (2021).
- [56] G. De las Cuevas, Tom Drescher, Tim Netzer, Quantum magic squares: dilations and their limitations, *J. Math. Phys.* **61**, 111704 (2020).
- [57] G. De las Cuevas, T. Netzer, I. Valentiner-Branth, Magic squares: Latin, Semiclassical and Quantum, preprint arXiv:2209.10230
- [58] D. Goyeneche, Z. Raissi, S. Di Martino, and K. Życzkowski, Entanglement and quantum combinatorial designs, *Phys. Rev. A* **97**, 062326 (2018).
- [59] B. Musto and J. Vicary, Orthogonality for quantum Latin isometry squares, *EPTCS* **287**, 253 (2019).
- [60] M. Grassl, T. Beth, and M. Rötteler, On optimal quantum codes, *Int. J. Quant. Inf.* **2**, 55 (2004).
- [61] G. Rajchel-Mieldzioc, *Quantum mappings and designs*, Ph.D. Thesis, Warsaw, September 2021, arXiv:2204.13008.
- [62] X.-D. Yu, T. Simnacher, N. Wyderka, H. C. Nguyen, and O. Gühne, A complete hierarchy for the pure state marginal problem in quantum mechanics, *Nat. Commun.* **12**, 1012 (2021).
- [63] S. Aravinda, S. A. Rather, and A. Lakshminarayan, From dual-unitary to quantum Bernoulli circuits: Role of the entangling power in constructing a quantum ergodic hierarchy, *Phys. Rev. Research* **3**, 043034 (2021).
- [64] L. Clarisse, S. Ghosh, S. Severini, and A. Sudbery, Entangling power of permutations, *Phys. Rev. A* **72**, 012314 (2005).
- [65] W. Bruzda, Structured Unitary Matrices and Quantum Entanglement, Ph.D. Thesis, Cracow 2021, arXiv:2204.12470.
- [66] A. Burchardt, Symmetry and Classification of Multipartite Entangled States, Ph.D. Thesis, Cracow 2021, arXiv:2204.13441.
- [67] B. Bertini, P. Kos, and T. Prosen, Exact correlation functions for dual-unitary lattice models in 1 + 1 dimensions, *Phys. Rev. Lett.* **123**, 210601 (2019).
- [68] B. Bertini, P. Kos, and T. Prosen, Operator Entanglement in Local Quantum Circuits I: Chaotic Dual-Unitary Circuits, *SciPost Phys.* **8**, 067 (2020).
- [69] S. A. Rather, S. Aravinda, and A. Lakshminarayan, Creating ensembles of dual unitary and maximally entangling quantum evolutions, *Phys. Rev. Lett.* **125**, 070501 (2020).
- [70] P. W. Claeys and A. Lamacraft, Ergodic and Nonergodic Dual-Unitary Quantum Circuits with Arbitrary Local Hilbert Space Dimension, *Phys. Rev. Lett.* **126**, 100603 (2021).
- [71] T. Benoist and I. Nechita, On bipartite unitary matrices generating subalgebra-preserving quantum operations, *Linear Algebra and Appl.* **521**, 70 (2017).
- [72] P. Facchi, G. Florio, U. Marzolino, G. Parisi, S. Pascazio, Multipartite entanglement and frustration, *N. J. Phys.* **12**, 025015 (2010).
- [73] P. Facchi, G. Florio, U. Marzolino, G. Parisi, S. Pascazio, Classical statistical mechanics approach to multipartite entanglement, *J. Phys. A* **43**, 225303 (2010).
- [74] M. Mestyán, B. Pozsgay, I. M. Wanless, Multi-directional unitarity and maximal entanglement in spatially symmetric quantum states, preprint arXiv:2210.13017
- [75] S. Brahmachari, R. N. Rajmohan, S. A. Rather, A. Lakshminarayan, Dual unitaries as maximizers of the distance to local product gates, preprint arXiv:2210.13307
- [76] A. Burchardt and Z. Raissi, Stochastic local operations with classical communication of absolutely maximally entangled states *Phys. Rev. A* **102**, 022413 (2020).
- [77] Z. Raissi, A. Burchardt, E. Barnes, General stabilizer approach for constructing highly entangled graph states, preprint arXiv:2111.08045
- [78] P. Facchi, G. Florio, G. Parisi, S. Pascazio and A. Scardicchio, A large- N approximated field theory for multipartite entanglement, *Phys. Rev. A* **92**, 062330 (2015).
- [79] B. D. McKay and I. M. Wanless, A census of small Latin hypercubes, *SIAM J. Discr. Math.* **22**, 719 (2008).
- [80] D.R. Stinson, *Combinatorial Designs: Constructions and Analysis*, New York: Springer, 2003.